

# Electrocatalysis of Organic Oxidations: Influence of Water Adsorption on the Rate of Reaction

T. Iwasita, X. H. Xia, H.-D. Liess, and W. Vielstich\*

*Institut für Physik, Universität der Bundeswehr München, Werner-Heisenberg-Weg 39, 85577 Neubiberg, Germany*

*Received: April 22, 1997; In Final Form: June 30, 1997*

Current/potential responses of small organic molecules show as a characteristic feature an increase in anodic current when changing the potential in the cathodic direction. In situ infrared data on the adsorption of methanol, formic acid, and water at Pt(111) are used to develop a new model explaining these well-known catalytic effects. Since the strength of water adsorption increases with increasing potentials above 0.4 V, the adsorption of organic molecules has to be considered as a water displacement reaction. The reaction rate is thus the result of the concurrence of two processes that are oppositely affected by the potential: the rate of oxidation (charge transfer) and the rate of adsorption. In situ IR data and cyclic voltammograms for the oxidation of methanol and formic acid on a Pt(111) surface are presented and discussed. For comparison, data on CO oxidation are presented.

## 1. Introduction

Small organic molecules such as formic acid, methanol, formaldehyde, etc., have often been taken as models in electrocatalysis. Apart from the specific properties inherent to the nature of the particular species under study, there are some common features in the electrocatalysis of these reactions which have no satisfactory explanation so far. Thus, most of these substances exhibit a current maximum during the application of an anodic polarization at Pt, which is also observed when the direction of the applied polarization is reversed, i.e., anodic currents are observed during polarization in the cathodic direction. At high anodic potentials ( $>0.8$  V at polycrystalline Pt), the current decays were explained in terms of the formation of a platinum oxide<sup>1,2</sup> and the increase in current during the polarization in the negative direction as due to the clean surface produced after reduction of the Pt oxide. This interpretation, however, cannot explain current decays observed at low anodic potentials, e.g., at 0.5 V for formic acid at polycrystalline Pt. Capon and Parsons<sup>3</sup> have shown that the same anodic peak was observed during the negative sweep when reversing the potential at, e.g., 0.75 V, before the formation of PtO. The same authors indicate that the process causing the anodic currents during the cathodic sweep must be one depending reversibly on potential and postulated the reversible formation of an intermediate of the type  $C(OH)_2$  as responsible for this behavior. For methanol in sulfuric acid solutions Markovic and Ross<sup>4</sup> suggested that sulfate adsorption, which is a reversible process, hinders the adsorption of organic species. Herrero et al.<sup>5</sup> suggested lateral sulfate–water interactions<sup>6,7</sup> to be responsible for the observed symmetric current/potential behavior during the oxidation of methanol. But it must be noticed that the reversible behavior described above is also observed in  $H_3PO_4$ <sup>5</sup> as well as in the presence of other less adsorbable electrolytes, such as  $HClO_4$ . Summarizing, no satisfactory explanation of the symmetric current–potential response has been given so far.

The application of spectroscopic methods together with the use of well-defined single-crystal surfaces shed some light in the complex pathways of organic oxidations. In particular

infrared spectroscopy data can be of very much help for understanding some features concerning the adsorption and oxidation of organic compounds, which are common to them all.

The role of adsorbed water upon organic oxidations will be analyzed here with the help of infrared data on the adsorption of water at Pt(111) in 0.1 M  $HClO_4$  solution. Potential-dependent bands for the OH stretching and HOH bending mode of water have recently been analyzed and interpreted in terms of the interaction of water molecules with the electric field of the double layer and with the metal surface.<sup>8</sup> Briefly, the shift of the bending mode at potentials in the range 0.4–0.9 V (Figure 1) is indicative of O-adsorbed water molecules suffering a progressive orientation of the molecular plane from a tilted to a perpendicular position. With increasing anodic potentials water dipoles acquire a configuration of minimum interaction energy with the electric field at the interface. This geometry causes an increasing participation of the  $3a_1$  orbital of water in the surface bond. This results in an increased HOH bond angle and, consequently, in a red-shift of the bending mode (see Figure 1). Water interaction with the Pt surface seems thus to be stronger than assumed so far. The interaction leads to a partial dissociation as observed in the case of several adsorbed weak acids. In this respect, it must be noted that the  $3a_1$  orbital has a partial bonding character in the intramolecular bond.<sup>9</sup> Since dissociation of water produces adsorbed OH, the interaction of water with the metal surface can play a deciding role in the electrocatalytic properties of the system.

In the present paper we discuss in particular the problem of the symmetric current–potential response during the oxidation of small organic molecules with the help of infrared spectroscopy results. For this purpose we have chosen  $CH_3OH$  and  $HCOOH$  as model molecules and Pt(111) as electrocatalytic material. The cyclic voltammetry response of CO is analyzed for comparison.

## 2. Experimental Section

**2.1. Solutions, Electrodes. Instrumentation.** Solutions were prepared with Millipore MilliQ water and analytical grade Merck chemicals. Spectra were taken using solutions of

\* Institut für Physikalische Chemie der Universität Bonn.

† Abstract published in *Advance ACS Abstracts*, August 15, 1997.

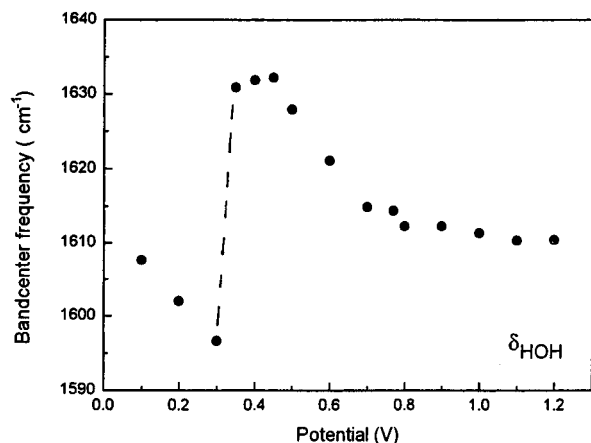


**Figure 1.** Potential dependence of the wavenumbers for the in-plane deformation (scissor mode) of water adsorbed at a Pt(111) electrode.<sup>8</sup>

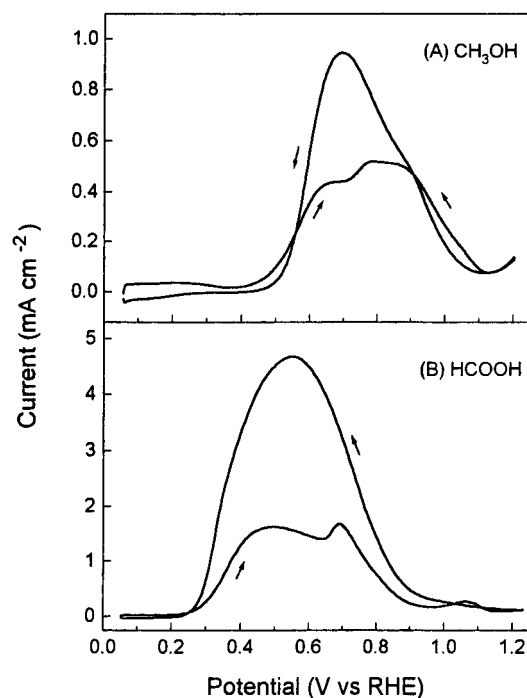


**Figure 2.** Cyclic voltammograms of a single-crystal Pt(111) electrode in 1 M CH<sub>3</sub>OH/0.1 M HClO<sub>4</sub> and 1 M HCOOH/0.1 M HClO<sub>4</sub>. Sweep rate 0.05V/s.

relatively high concentration (1 M) of HCOOH or CH<sub>3</sub>OH in order to minimize the problem of reactant depletion in the thin layer.

The Pt(111) single-crystal electrode used for the IR measurements has a surface area of 0.64 cm<sup>2</sup>. After flame-annealing and cooling in a H<sub>2</sub>/Ar stream the probe was contacted with a drop of water, saturated with the gas mixture, and transferred to the spectroelectrochemical cell.

FTIR spectra were measured with a Bruker IFS 66 spectrometer, equipped with a Globar source and a mercury–cadmium–telluride (MCT) detector. The IR cell was provided with a CaF<sub>2</sub> prismatic (60°) window.

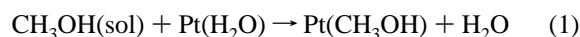
**2.2. Experimental Procedure.** After immersion of the probe into the 0.1 M HClO<sub>4</sub> solution a test voltammogram in meniscus configuration was taken. After this the electrode was immersed in the test solution, and the potential was set to 0.05 V. The solution was then replaced by the organic electrolyte (HCOOH, CH<sub>3</sub>OH), while keeping the working electrode at 0.05 V. Then the sample was gently pressed against the IR window, and 256-scan spectra were taken at potentials in the range 0.05–

0.9 (or 1.2) V RHE, during the application of steps to more positive potentials and back to the initial potential.

### 3. Results and Discussion

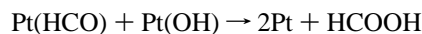
Cyclic voltammograms for methanol and formic acid oxidation at Pt(111) are shown in Figure 2 A,B. These voltammograms exhibit anodic current maxima during the anodic as well as the cathodic sweep direction. They typically illustrate the behavior of other small organic molecules such as formaldehyde,<sup>2</sup> ethanol,<sup>11,12</sup> etc. This *symmetric* current–potential behavior will be discussed below for the cases of methanol and formic acid.

**3.1. Methanol.** The main reaction path during the oxidation methanol is the formation of CO<sub>2</sub> via CO as intermediate. To a minor extent HCOOH is formed in a parallel reaction. The reaction pathway via CO can be schematically described as follows:



The first step represents the adsorption of a methanol molecule on a Pt site which is initially occupied by a water molecule. Dissociative adsorption (2) can occur only if methanol molecules come in contact with the metal atoms. Being aware of the strength of the H<sub>2</sub>O/Pt(111) interaction at potentials above ca. 0.45 V,<sup>8</sup> eq 1 emphasizes that adsorption must be considered as a water replacement reaction.<sup>12</sup> After adsorption, methanol undergoes dehydrogenation reactions in several fast steps forming partially hydrogenated intermediates and CO<sup>13,14</sup> (eq 2). Oxidation of the CO adsorbate requires the dissociation of water to form Pt(OH), (eq 3). This step is currently postulated in the oxidation mechanism of methanol and other organic compounds. IR results on water adsorption<sup>8</sup> suggest the possibility of (OH)<sub>ad</sub> formation as the H<sub>2</sub>O/Pt interaction seems to be stronger than formerly assumed. A band at ca. 3270 cm<sup>-1</sup>, observed at potentials higher than 0.5 V in the spectra of adsorbed water was tentatively assigned to an adsorbed (OH) species.<sup>8</sup> Thus above ca. 0.45 V oxidation to CO<sub>2</sub> can occur.

Above 0.45 begins also the formation of HCOOH. The corresponding pathway may include one of the intermediates formed during the dehydrogenation steps (2) and will be formally written as<sup>13</sup>



For the purpose of the present discussion the nature of the intermediate forming formic acid is irrelevant. HCOOH itself can be further oxidized to CO<sub>2</sub>. Note that the onset of the current producing the first peak in the voltammogram coincides with the threshold potential for both CO<sub>2</sub> and HCOOH formation.

Increasing the potential results in two opposite effects on the reactions given above. The oxidation of CO or of any of the intermediates to form CO<sub>2</sub> (or HCOOH) is favored by charge transfer and water dissociation to form Pt(OH) with increasing positive potential. On the other hand, an increase in potential causes a stronger H<sub>2</sub>O–Pt interaction and hinders the water displacement by methanol.

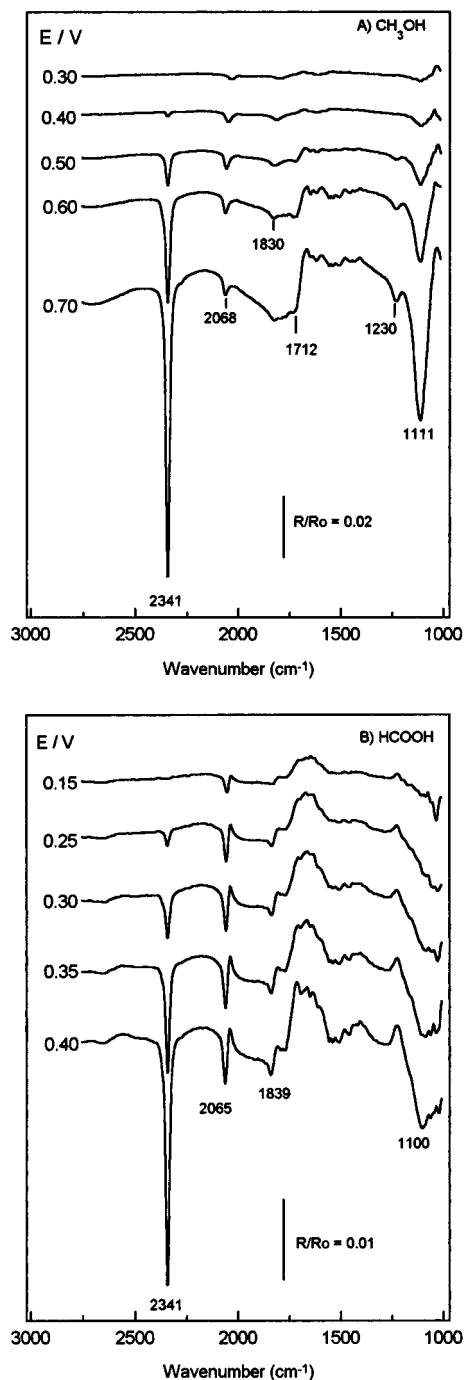


**Figure 3.** In situ FT infrared reflectance spectra from a Pt(111) electrode for (A) 1 M  $\text{CH}_3\text{OH}/0.1$  M  $\text{HClO}_4$  and (B) 1 M  $\text{HCOOH}/0.1$  M  $\text{HClO}_4$ . Sample potentials as indicated; the reference spectra were taken at 0.05 V; 256 interferometer scans were averaged at each potential.

The effects described above can be reversed by reversing the direction of the potential sweep as in a cyclic voltammogram, giving rise to the "symmetric" current–potential response presented in Figure 2. As shown below, the results of IR measurements correlate well with this interpretation.

A series of spectra were taken in a 1 M  $\text{CH}_3\text{OH}/0.1$  M  $\text{HClO}_4$  solution. Following the procedure discussed in the experimental part, spectra were collected during the application of potential steps from 0.05 to 0.9 V and then back to the initial potential. Figure 3A shows some spectra out of this series. As stated in the experimental part, the procedure used here allowed us to monitor the initial stages of methanol adsorption.<sup>14</sup>

The bands observed at 2068 and 1830  $\text{cm}^{-1}$  correspond

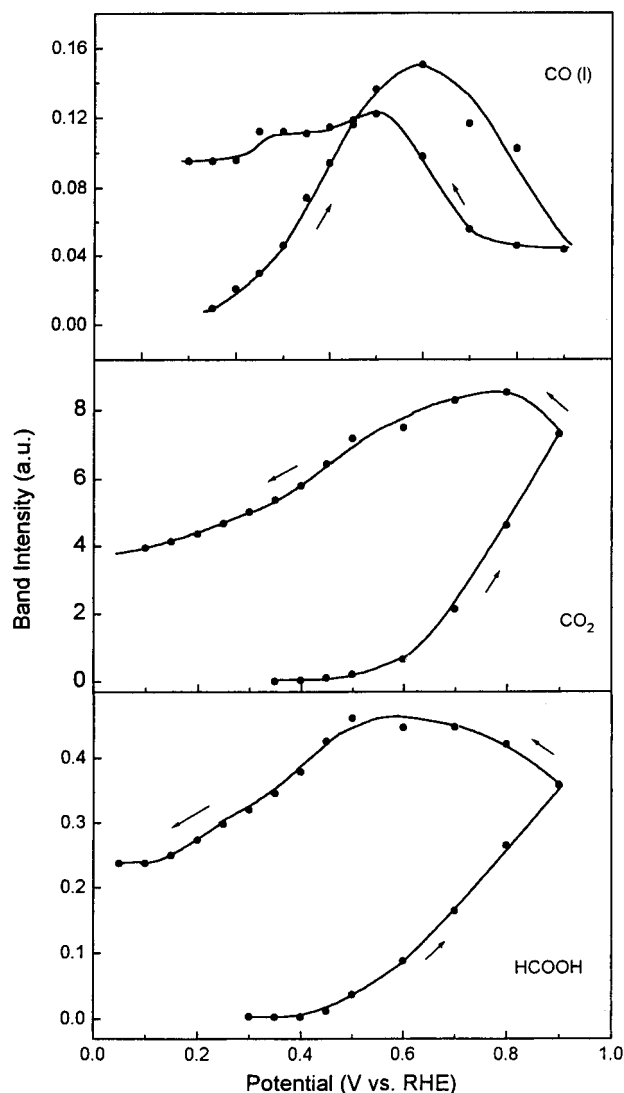


**Figure 4.** Potential dependence of the integrated band intensity for linear bonded CO,  $\text{CO}_2$ , and HCOOH from spectra taken during the electrooxidation of methanol as indicated in Figure 2.

respectively to linearly and bridge-bonded CO and that at 2341  $\text{cm}^{-1}$  to  $\text{CO}_2$ . The intensities of the features for CO and  $\text{CO}_2$  can be used to monitor methanol adsorption and oxidation respectively, i.e., these features represent the two processes with opposite potential dependence referred to above. The band at 1230  $\text{cm}^{-1}$  is due to methyl formate<sup>14</sup> produced via a homogeneous reaction of methanol with formic acid. Its intensity is therefore proportional to the amount of HCOOH formed in a lateral reaction. A plot of the respective band intensities is given in Figure 4.

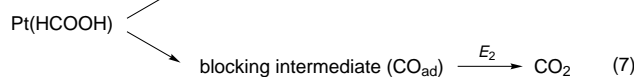
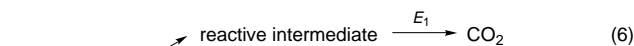
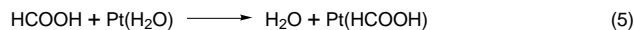
We observe the growth of the CO signal from ca. 0.15 V to a maximum at about 0.6 V, after which it decays. At increasing potentials above this value, carbon monoxide can be oxidized at a higher rate, but the adsorption of methanol from the bulk is unable to restore the concentration of surface species. However it should be observed that after inverting the direction of the potential steps, the  $\text{CO}_2$  and HCOOH signals *grow* in accordance with the increase in current during the cathodic scan, but the CO band intensity *also grows*. Thus the observation indicates an increased rate of CO formation, which can occur only by increasing the rate of methanol adsorption (eq 1). These results emphasize the blocking capacity of the  $\text{Pt}(\text{H}_2\text{O})\text{--Pt}(\text{OH})$  layer. We suggest that in the cathodic scan, under the conditions where both  $\text{CO}_2$  and CO signals grow (up to 0.7 V) methanol

adsorption (i.e., water displacement, eq 1) is the rate-limiting step. Further decrease in potential causes a faster increase of methanol adsorption and a parallel decrease of CO<sub>2</sub> production. This decay, observed in the cathodic sweep as the potential decreases below 0.7 V, is the result of two effects which are in fact interrelated: (a) the decrease of the rate of electron transfer (and concomitant with this, the production of Pt(OH)) and (b) the accumulation of CO at the surface. The decrease of CO at 0.25 V is probably due to conversion to bridge-bonded CO.

It should be noted that there is a parallel behavior between CO<sub>2</sub> and HCOOH production as Figure 4 shows, both beginning at ca. 0.4 V, i.e., at the onset of current in the voltammogram of Figure 2A. The increase of the band intensities during the negative potential scan is relatively poor in comparison with the well-defined current increase in the voltammogram. This may be caused by the partial methanol depletion in the thin layer as well as by an increased rate of CO<sub>2</sub> and HCOOH diffusion to the solution outside, after several minutes of electrolysis. The diffusion is also suggested by the approximately  $t^{-1/2}$  decay of both signals as their production ceases at potentials below 0.5 V. From this point of view, the thin-layer configuration used in the in situ FTIR technique complicates the observation of the time response for soluble species. The growing of CO<sub>2</sub> and HCOOH during the reverse scan is a well-proven result as shown by on-line mass spectrometry.<sup>15</sup>

There are, obviously, some complexities in the reaction, which cannot be explained so far. However the results presented here highlight the role of water in the methanol oxidation process.

**3.2. Formic Acid.** The electrooxidation of formic acid has been described in terms of a "dual" path mechanism.<sup>3,16,17</sup> For the purpose of our discussion we reformulate this mechanism as follows, including the adsorption reaction:



With potential  $E_2 \gg E_1$ ; these reactions are called the *fast* (or direct) and *slow* pathway, respectively.

The fast reaction pathway is the main process taking place under the first maximum of the voltammogram (Figure 2B). This maximum is observed as a 0.43 V well-defined peak in a 0.1 M HCOOH solution.<sup>17</sup> In the present case, the voltammogram was taken in a 1 M HCOOH solution, and the potential scan was started after exchanging the electrolyte at 0.05 V. This operation required ca. 3 min, which was approximately the time elapsed in the IR experiment before starting spectra collection. Under these conditions some poisoning of the surface occurs already at the initial potential (0.05 V), which lowers the height of the positive going maximum with respect to the negative going one. At the same time the first maximum broadens and shifts to ca. 0.5 V. The second maximum, at about 0.7 V, corresponds to the slow pathway, i.e., to the oxidation of the adsorbate carbon monoxide. Reversing the potential after the current falls to very low values at 1.2 V, causes a reactivation of the reaction and the current grows again toward a maximum at ca. 0.6 V.

It is interesting to observe that using the Pt(111) surface the *symmetric* current response is also observed if the potential scan is reversed short after the first peak, as in the experiment of Figure 5. A similar behavior was reported by Capon and Parsons for polycrystalline platinum.<sup>3</sup> Thus the process responsible for the current decay at the first peak depends

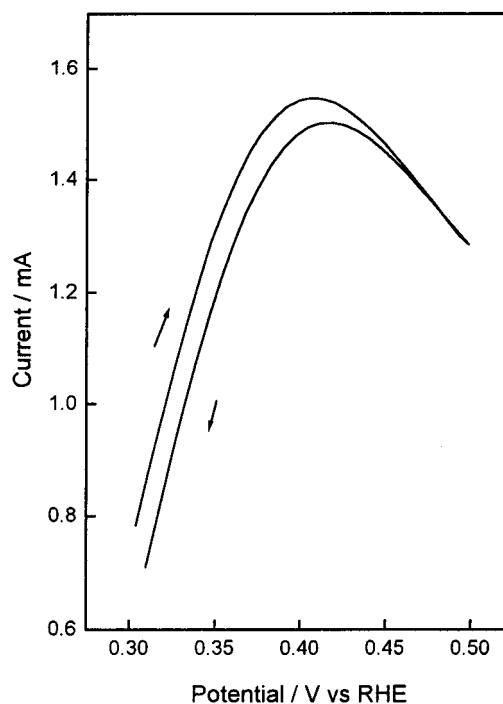


**Figure 5.** Cyclic voltammogram for a Pt(111) electrode in 0.1 M HCOOH/0.1 M HClO<sub>4</sub>. The direction of potential scan is reversed at 0.5 V. Sweep rate: 0.05 V/s.

reversibly on the potential. As in the case of methanol we assume that a stronger H<sub>2</sub>O–Pt interaction is unfavorable for HCOOH adsorption (eq 5) and causes the decay of current at the first maximum.

A series of spectra were taken in a 1 M HCOOH/0.1 M HClO<sub>4</sub> solution from 0.05 to 1.2 V and then back to the initial potential. Some selected spectra out of this series are shown in Figure 3B. We observe bands at ca. 2065 and 1839 cm<sup>-1</sup> due to linear and bridge-bonded CO respectively and a strong band at 2341 cm<sup>-1</sup> corresponding to the reaction product CO<sub>2</sub>.

In Figure 6 the integrated band intensities for both CO species and CO<sub>2</sub> are presented. Due to the bipolar character of the CO features (see Figure 3B) the integration was performed after recalculating the spectra with a reference spectrum at 1.1 V. The band for bridge bonded CO overlaps considerably with the positive going carbonyl band of HCOOH at 1730 cm<sup>-1</sup> and could not be evaluated in the whole potential range.

The onset of HCOOH oxidation via the direct reaction pathway (eq 6) is indicated by the beginning of CO<sub>2</sub> production shortly above 0.2 V, i.e., well below the beginning of CO oxidation. The band intensity for linear bonded CO grows with the potential up to a maximum at 0.5 V and then decays almost to zero at 1.0 V. Reversing the potential after reaching 1.2 V causes the CO signal to increase again. At the same time, the CO<sub>2</sub> production also increases. Obviously, there must be an increase in the rate of HCOOH adsorption due to a decreased H<sub>2</sub>O–Pt interaction as explained in the case of methanol. Here, again, the water displacement reaction plays the deciding role.

As with the methanol experiment, the increase in the CO<sub>2</sub> signal during the application of negative going steps is relatively poor and does not correlate with the pronounced increase in current observed in the voltammogram. The consumption of HCOOH in the thin layer and the fast CO<sub>2</sub> diffusion as its concentration increases at high anodic potentials may cause this effect. Note the decay ( $\sim t^{-1/2}$ ) of CO<sub>2</sub> as the reaction rate becomes very low at potentials below 0.35 V.

**3.3. Adsorption Energies Involved. Comparison of the CV Responses of Small Organic Molecules with That of CO.**

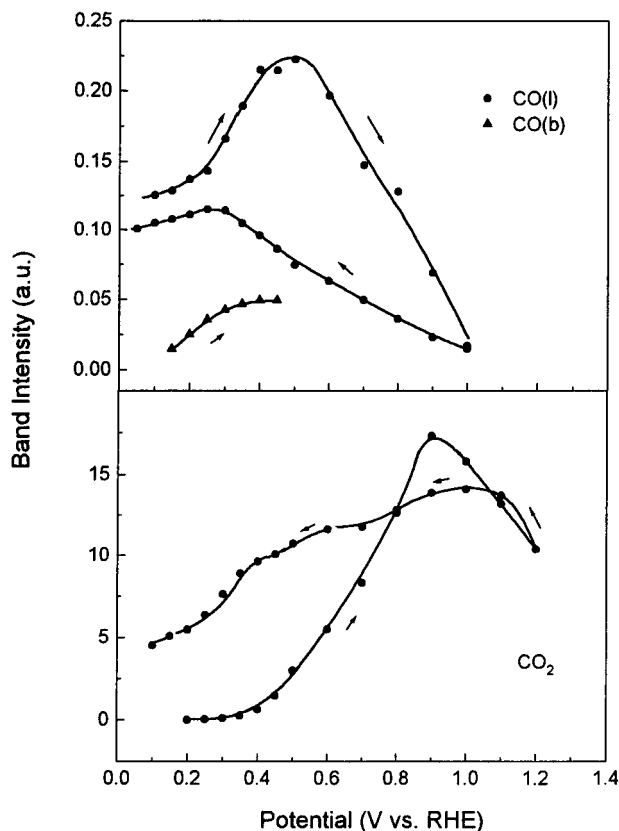


**Figure 6.** Potential dependence of the integrated band intensity for CO and CO<sub>2</sub> from spectra taken during the electrooxidation of formic acid as indicated in Figure 3.

Our model for the oxidation of small organic molecules emphasizes the adsorption process as one where the organic species has to compete with water for the adsorption site. In other words we assume that there is an energy barrier for the desorption of water, which is comparable with that of the organic species.

A rough estimation of the adsorption energies involved can be accomplished from TDS data from the gas phase since the desorption temperature can be used to calculate the respective energy of adsorption. Pt(111) show a chemisorbed state for water at 165–170 K. From these data and assuming a first-order kinetic and a preexponential factor of  $10^{-13} \text{ s}^{-1}$ , the chemisorption bond strength of water was estimated to be about 42 kJ/mol. For CH<sub>3</sub>OH and HCOOH, TDS data at Pt(111) show molecular desorption at 180<sup>18</sup> and 170 K,<sup>19</sup> respectively. Accordingly, the adsorption energy for the molecular (undissociated) species must be of the same order as that of water. Contrasting with these low values, the energy of adsorption of carbon monoxide, calculated from TDS data lies in the order of 108 kJ/mol (26 kcal/mol<sup>20</sup>). The adsorption energy is a measure for the molecule–metal interaction. If we assume that the same relationship as in UHV holds for the energy of interaction with the surface in the electrochemical environment, a competition with water for Pt sites can be expected from the organic molecules *but not from CO*. From this point of view, according to our model, no increase in current should be observed during the cathodic scan in a CO containing solution. This effect, i.e., the absence of a “reactivation peak” has been shown in voltammograms at polycrystalline<sup>21</sup> and single-crystal Pt<sup>22</sup> in CO-saturated solutions. The current–potential curve of Figure 7 was taken in 0.1 M HClO<sub>4</sub>/CO-saturated solution after adsorption during 4 min at 0.05 V. The features observed during the positive going scan have been explained in detail by Caram et al.<sup>21</sup> for polycrystalline Pt and Wieckowski et al.<sup>22</sup> for single-

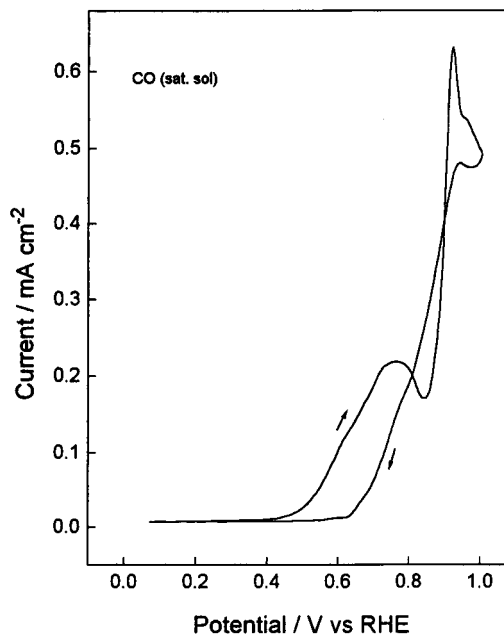


**Figure 7.** Current–potential curves for a Pt(111) electrode in saturated CO/0.1 M HClO<sub>4</sub> solution. Sweep rate: 10 mV/s.

crystal Pt surfaces and will not be discussed here. For the purpose of the present discussion, we observe that only a decrease of the current below 0.9 V occurs during the reverse scan, according to the expected behavior for a system governed by the rate of charge transfer. The adsorbed water layer does not represent a barrier for CO adsorption and oxidation.

#### 4. Concluding Remarks

The discussion above stresses the dual role played by water in the electrocatalysis of organic oxidations. On one side, water is the reaction partner supplying the necessary oxygen for the complete oxidation of one-O-atom intermediates. On the other side, this interaction is just the reason for an inhibition of the reaction at increasing positive potentials. These two opposite effects can explain that during a cyclic voltammogram, independently of the direction of the applied potential, only anodic current maxima occur.

**Acknowledgment.** Financial support by the Deutsche Forschungsgemeinschaft (DFG) and the Fonds der Chemischen Industrie is gratefully acknowledged.

#### References and Notes

- (1) Giner, J. *Ber. Bunsen-Ges. Phys. Chem.* **1959**, *63*, 386.
- (2) Vielstich, W. *Fuel Cells*; Wiley-Interscience: New York, 1970.
- (3) Capon A.; Parsons, R. *J. Electroanal. Chem.* **1973**, *45*, 205.
- (4) Markovic, N.; Ross, P. N. *J. Electroanal. Chem.* **1992**, *330*, 499.
- (5) Herrero, E.; Franaszczuk, K.; Wieckowski, A. *J. Phys. Chem.* **1994**, *98*, 5074.
- (6) Magnussen, O. M.; Hageböck, J.; Hotlos, J.; Behm, R. J. *Faraday Discuss.* **1992**, *94*, 329.
- (7) Edens, G. J.; Gao, X.; Weaver, M. J. *J. Electroanal. Chem.* **1994**, *375*, 357.
- (8) Iwasita T.; Xia, X. H. *J. Electroanal. Chem.* **1996**, *411*, 95.
- (9) Thiel, P. A.; Madey, T. E. *Surf. Sci. Rep.* **1987**, *7*, 211.
- (10) Chang, S.-C.; Leung, L.-W. H.; Weaver, M. J. *J. Phys. Chem.* **1990**, *94*, 6013.
- (11) Xia X. H.; Liess, H.-D.; Iwasita, T. *J. Electroanal. Chem.*, in press.
- (12) Trasatti, S. *Proceedings of the Symposium The Chemistry and Physics of Electrocatalysis*; The Electrochemical Society: Pennington, NJ, 1984; Vol. 84–12, p 150.
- (13) Bagotzki, V. S.; Vassiliev, Yu. B.; Khazova, O. A. *J. Electroanal. Chem.* **1977**, *81*, 229.
- (14) Xia, X. H.; Iwasita, T.; Ge, F.; Vielstich, W. *Electrochim. Acta* **1996**, *41*, 711.

- (15) Iwasita, T. In *Advances in Electrochemical Science and Engineering*; Gerischer H., Tobias, C., Eds.; Verlag Chemie: Weinheim, 1990; Vol. 1, p 127.
- (16) Breiter, M. *Electrochemical Processes in Fuel Cells*; Springer-Verlag: Berlin, 1969.
- (17) Iwasita, T.; Xia, X. H.; Herrero, E.; Liess, H.-D. *Langmuir* **1966**, 12, 4260.
- (18) Sexton, B. A. *Surf. Sci.* **1981**, 102, 271.
- (19) Columbia M. R.; Thiel, P. *Surf. Sci.* **1990**, 235, 53.
- (20) Mc. Cabe R. W.; Schmidt, L. D. *Surf. Sci.* **1977**, 66, 101.
- (21) Caram J. A.; Gutiérrez, C. *J. Electroanal. Chem.* **1991**, 305, 259.
- (22) Wieckowski, A.; Rubel, M; Gutiérrez, C. *J. Electroanal. Chem.* **1995**, 382, 9722.